Proceedings of the 8th IEEE Mediterranean Conference
on Control and Automation (MED 2000)
Rio, Patras, GREECE 17-19 July, 2000

Reduced-Order Model Matching Control Design for Gantry Robots*

Xuedong Yang and David G. Taylor

Georgia Institute of Technology
School of Electrical and Computer Engineering
Atlanta, GA 30332-0250 USA

Abstract: An important application of gantry robots is circuit board assembly, a challenging task involving rapid point-to-point motions that tend to induce structural vibrations. Attempts to suppress such vibrations through model-based controller design must take into account the variation of the flexible dynamics with respect to placement head position. To circumvent the time-varying configuration-dependent mass distribution property of the flexible dynamics, this paper explores the potential of a controller design based instead on the rigid dynamics. This reduced-order approach to controller design is recommended for gantry robots with relatively stiff beams, since it offers an appropriate compromise between modeling/implementation requirements and performance potential. The proposed reduced-order controller is designed using a model-matching formulation to adjust the transient response, and an integral effect is included to reject friction force disturbances for satisfactory steady-state response. The reduced-order model matching controller has been implemented and tested on a prototype gantry robot. The experimental results confirm the viability of the new design and show its superiority over the more traditional PID controller.

Keywords: Gantry robots, flexible beams, structural vibration, point-to-point motion, reduced-order control, model matching control.

1 Introduction

Gantry robots are used for a wide variety of manufacturing tasks, including circuit board assembly [5]. In such applications, gantry robots provide primarily two motion axes, a beam sliding along a frame and a head sliding along the beam. The motion control sensors typically found on gantry robots are joint-mounted linear encoders that measure the positions of the two axes. In such point-to-point motion control applications, the goal is to move the gantry head to the target position as fast as possible yet also settle quickly with μm accuracy. Unless the control system is carefully designed, attempts for rapid positioning will excite structural vibrations [3] in the gantry beam due to its finite stiffness, thus leading to unacceptably large settling times or even instability.

A question that arises in model-based control design is what level of model complexity is really required for control design purposes? Generally speaking, it is wise to design the control system using the simplest possible model that yields closed-loop stability and acceptable performance. Considering specifically the gantry robot application, the design model could range from a simple rigid model to the more complex flexible models that include higher-order modes of vibration. Since the gantry head moves along the gantry beam, the flexible models possess a time-varying configuration-dependent mass distribution and, consequently, the design of high performance controllers for the relatively flexible beam case remains a challenging and unsolved problem. This paper focuses instead on the relatively stiff beam case (see also [4]), which is perhaps more relevant to present-day industrial applications, and the primary objective is to determine how well one can do by using just the rigid model for control design purposes.

The rigid model, or reduced-order, approach to controller design is recommended for gantry robots with relatively stiff beams because it offers an appropriate compromise between modeling/implementation requirements and performance potential. The proposed reduced-order controller is designed using a model-matching formulation to

*This work was supported in part by the National Science Foundation under grant ECS-9158037 and by Siemens AG.

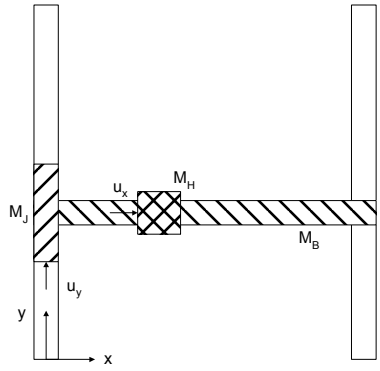

Figure 1: Top view of gantry robot.

adjust the transient response, and an integral effect is included to reject friction force disturbances for satisfactory steady-state response [1]. The resulting second-order compensator includes feedforward and feedback components, and is programmed using five coefficients: the damping ratio and natural frequency of the reference model; two free parameters that determine the location of stable pole-zero cancellations; and moving mass.

The reduced-order model matching controller has been implemented and tested on a prototype gantry robot. The prototype uses rotary motors and belt-pulley transmissions to provide the driving forces. The actuator dynamics introduced by the transmission elasticity are compensated by a stiffening feedback loop [2]. The experimental results confirm the viability of the new design and show its superiority over the more traditional PID controller.

2 Gantry Robot Modeling

2.1 Basic Description

A simplified sketch of the gantry robot is provided in Fig. 1. Two stationary rails guide the motion of a moving beam, and this moving beam serves as the guideway for the moving head. Motion of the beam is actuated and constrained by the joint located at the left end of the beam; this joint is also where the position sensor is typically located.

The motion control task involves repositioning the head, which has coordinates $(x_h(t), y_h(t))$, from some initial point (x_i, y_i) to some final point (x_f, y_f). Because the beam has finite stiffness, the input force $u_y(t)$ will tend to excite bending vibrations, and thus the x-coordinate of the head $x_h(t)$ significantly affects the dynamic response of the y-coordinate of the head $y_h(t)$. On the other hand, the x-axis dynamics are essentially rigid and decoupled from the y-axis dynamics. Hence, for the purposes of this paper, it suffices to focus on beam motions (for various fixed head positions) and consequently the input force $u_y(t)$ in Fig. 1 will be denoted simply by $u(t)$ from this point forward.

2.2 Rigid Model

As pointed out earlier, this paper is concerned with the design of model matching controllers using the reduced-order rigid-body model of the gantry robot. From Fig. 1, it should be clear that beam motions require acceleration of the total mass $M = M_J + M_B + M_H$, where M_J denotes joint mass, M_B denotes beam mass and M_H denotes head mass. Hence, the rigid-body dynamics may be easily written as

$$M\ddot{y}(t) = u(t) - f(t) \tag{1}$$

where $u(t)$ is the input force, $f(t)$ is a friction disturbance force, and $y(t)$ denotes the position of the rigid-body system. Note that, due to rigid-body approximation, there is no distinction between the coordinates of different points along the beam and, therefore, in (1) the subscript h has been dropped and $y(t)$ represents simply the axis position. Furthermore, this rigid model clearly exhibits no dependence on the head position, implying that controllers designed using this rigid model will require neither measurement of, nor scheduling with respect to, head position. Although the more accurate flexible model of a gantry robot [5] is an LTV system, the simpler rigid model is an LTI system.

3 Model Matching Control Design

3.1 Background

The approach to control design recommended in this paper is based on model matching, whereby the designer specifies directly an admissible closed-loop transfer function and then synthesizes the compensation scheme that provides the desired result. The advantage of model matching design over the more classical design methods is that trial-and-error design iterations are avoided, and both stability and performance can be predicted in advance from the reference model specification, provided of course that the plant model used in the design process is sufficiently accurate.

The theory of model matching design for single-input, single-output, LTI systems is described in [1]. Given an open-loop plant transfer function $G(s)$ with coprime numerator and denominator polynomials, a desired closed-loop transfer function $G_d(s)$ is said to be implementable if a control system can be designed that meets the following constraints: all compensators used have proper rational transfer functions; the resulting system is well-posed and internally stable; and all forward paths from reference input to controlled output pass through the plant. By enforcing these constraints, the design will be realizable and will avoid amplification of high-frequency noise and unstable pole-zero cancellations. The necessary and sufficient conditions for implementability are as follows: the relative degree

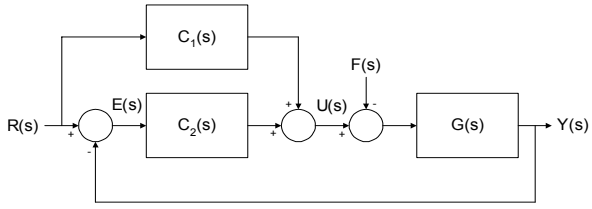

Figure 2: Structure of control system.

of $G_d(s)$ must be greater than or equal to the relative degree of $G(s)$; all nonminimum-phase zeros of $G(s)$ must be retained in $G_d(s)$; and $G_d(s)$ must be stable.

The rigid model transfer function from input force to output position is given by

$$G(s) = \frac{1}{Ms^2} \tag{2}$$

and thus an implementable choice of reference model $G_d(s)$, in the sense defined above, would be any stable transfer function having relative degree no smaller than two. The lowest order choice would therefore be the second-order relative-degree-two transfer function

$$G_d(s) = \frac{\omega_d^2}{s^2 + 2\zeta_d\omega_d s + \omega_d^2} \tag{3}$$

which is parameterized by (ζ_d, ω_d) for ease of setting performance specifications. By fixing ζ_d on the basis of overshoot, ω_d may be adjusted to provide any desired settling time for the reference model response.

3.2 Feedforward/Feedback Configuration

With both $G(s)$ and an implementable $G_d(s)$ available, attention now turns to the issue of selecting an appropriate configuration for the control system. The unity-feedback configuration, though commonly employed, is only sufficient for modifying pole locations. To place both poles and zeros, as required for general model matching, a configuration that includes a feedforward path is needed. This fact is easily established by considering the configuration shown in Fig. 2. The relationship between the reference input and the plant output is found to be

$$Y(s) = \frac{(C_1(s) + C_2(s))\,G(s)}{1 + C_2(s)G(s)}R(s) \tag{4}$$

The denominator shows that the feedback compensator $C_2(s)$ may be used to place the poles of the closed-loop system. The numerator shows that the feedforward compensator $C_1(s)$ is needed to place the closed-loop zeros once the feedback compensator has been designed.

To examine the constraints imposed by model matching, it is useful to express all transfer functions in terms of their numerator and denominator polynomials. To this end, the plant and reference model may be generally denoted by

$$G(s) = \frac{N(s)}{D(s)} \qquad G_d(s) = \frac{N_d(s)}{D_d(s)} \tag{5}$$

and the two compensators may be generally denoted by

$$C_1(s) = \frac{B_1(s)}{A(s)} \qquad C_2(s) = \frac{B_2(s)}{A(s)} \tag{6}$$

where, without loss of generality, both compensators have been assumed to share the same denominator polynomial. Using these notations and the closed-loop transfer function from (4), the model matching constraint may be generally written as

$$\frac{N(s)\,(B_1(s) + B_2(s))}{D(s)A(s) + N(s)B_2(s)} = \frac{N_d(s)}{D_d(s)} \tag{7}$$

For the specific choices of $G(s)$ and $G_d(s)$ in (2) and (3), this model matching constraint reduces to

$$\frac{B_1(s) + B_2(s)}{Ms^2A(s) + B_2(s)} = \frac{\omega_d^2}{s^2 + 2\zeta_d\omega_d s + \omega_d^2} \tag{8}$$

The remainder of this section provides a possible design for polynomials $A(s)$, $B_1(s)$ and $B_2(s)$ based on model matching constraint (8).

3.3 Second-Order Matching Design

A second-order compensator is the lowest order proper compensator that is capable of providing zero steady-state error in the presence of friction force disturbances. The compensator polynomials will have the form

$$A(s) = a_0 + a_1 s + a_2 s^2 \tag{9}$$
$$B_1(s) = b_{10} + b_{11} s + b_{12} s^2 \tag{10}$$
$$B_2(s) = b_{20} + b_{21} s + b_{22} s^2 \tag{11}$$

where the coefficients are to be determined. Considering (8), it is clear that both polynomial degrees on the left-hand side exceed those on the right-hand side by two. Hence, model matching will require two stable pole-zero cancellations on the right-hand side of (8). Multiplying both the numerator and denominator of the right-hand side of (8) by the common factor $s^2 + \alpha s + \beta$, where $\alpha > 0$ and $\beta > 0$ are design parameters, the process of matching polynomial coefficients yields 8 equations for 9 variables. An additional constraint is obtained by insisting that the compensator have a pole at the origin, resulting in

$$a_0 = 0 \tag{12}$$
$$a_1 = M^{-1}\,(2\zeta_d\omega_d + \alpha) \tag{13}$$
$$a_2 = M^{-1} \tag{14}$$
$$b_{10} = 0 \tag{15}$$

$$b_{11} = -2\zeta_d\omega_d\beta \quad (16)$$
$$b_{12} = -(2\zeta_d\omega_d\alpha + \beta) \quad (17)$$
$$b_{20} = \omega_d^2\beta \quad (18)$$
$$b_{21} = \omega_d^2\alpha + 2\zeta_d\omega_d\beta \quad (19)$$
$$b_{22} = \omega_d^2 + 2\zeta_d\omega_d\alpha + \beta \quad (20)$$

This compensator may be implemented in the time-domain using the realization

$$\dot{x}_C(t) = A_C x_C(t) + B_{C1} r(t) + B_{C2} e(t) \quad (21)$$
$$u(t) = C_C x_C(t) + D_{C1} r(t) + D_{C2} e(t) \quad (22)$$

where

$$A_C = \begin{bmatrix} 0 & 1 \\ 0 & \lambda \end{bmatrix} \quad (23)$$
$$B_{C1} = \begin{bmatrix} b_{11} + b_{12}\lambda \\ b_{10} + b_{11}\lambda + b_{12}\lambda^2 \end{bmatrix} \quad (24)$$
$$B_{C2} = \begin{bmatrix} b_{21} + b_{22}\lambda \\ b_{20} + b_{21}\lambda + b_{22}\lambda^2 \end{bmatrix} \quad (25)$$
$$C_C = M \begin{bmatrix} 1 & 0 \end{bmatrix} \quad (26)$$
$$D_{C1} = Mb_{12} \quad (27)$$
$$D_{C2} = Mb_{22} \quad (28)$$

and $\lambda = -a_1/a_2$. This design requires implementation of a single second-order filter, even though both feedforward and feedback compensation are used.

4 Compensation for Belt Transmission

If the gantry robot is not equipped with direct-drive linear motors, the assumption that $u(t)$ is the force input for the plant is no longer valid. Rotary-to-linear transmissions introduce actuator dynamics that must be considered if fast motion is desired. This section provides a methodology for modifying the previously designed force control $u(t)$ to account for the elasticity effects of belt-pulley transmissions [2].

As shown in [5], if a belt-pulley transmission is used to provide the driving force to the gantry robot mass, then a more accurate model for control design purposes is

$$M\ddot{y}(t) = k(\rho\theta(t) - y(t)) \quad (29)$$
$$J\ddot{\theta}(t) = -\rho k(\rho\theta(t) - y(t)) + T(t) \quad (30)$$

where $\theta(t)$ is the motor angular position, ρ is the pulley radius, J is the total inertia of the motor and driving pulley and k is the stiffness of the belt. In this model the control input is $T(t)$, the motor torque, and the driving force is now provided through an elastic coupling. The elastic displacement is defined by

$$z(t) = \rho\theta(t) - y(t) \quad (31)$$

and has open-loop dynamics

$$\ddot{z}(t) = a_z z(t) + b_z T(t) \quad (32)$$

where

$$a_z = -k\left(\frac{\rho^2}{J} + \frac{1}{M}\right) \qquad b_z = \frac{\rho}{J} \quad (33)$$

If $z(t)$ can be measured, i.e. if both $y(t)$ and $\theta(t)$ can be measured, then it is possible to use $z(t)$ feedback to improve the response of $z(t)$ so that $kz(t)$, the elastic force, might be at all times approximately equal to the control force $u(t)$ already designed. To this end, choose the motor torque $T(t)$ according to

$$b_z T(t) = \frac{k_0}{k}u(t) - (a_z + k_0)\, z(t) - k_1\dot{z}(t) \quad (34)$$

where $k_0 > 0$ and $k_1 > 0$ are design coefficients. The result of this choice is the closed-loop elastic system

$$\ddot{z}(t) + k_1\dot{z}(t) + k_0 z(t) = \frac{k_0}{k}u(t) \quad (35)$$

Appropriate choice of k_0 and k_1 on the basis of rise-time and overshoot will allow the quasi-steady-state conclusion

$$kz(t) \approx u(t) \quad (36)$$

i.e. that the compensated flexible transmission responds almost like an ideal rigid transmission. Since (34) represents a modification to the original motion control $u(t)$ rather than a complete redesign, this approach to transmission compensation has the benefit of modularity.

5 Experimental Results

The reduced-order model matching (RMM) controller with belt transmission compensation has been tested experimentally on a prototype gantry robot, similar to those used commercially for circuit board assembly. The beam has length $l = 0.8$ m and the range of head motion is $x_h \in [0.14\text{ m},\ 0.7\text{ m}]$. The masses are $M_J = 7.41$ kg, $M_B = 7.57$ kg and $M_H = 8.72$ kg. The transmission is characterized by stiffness $k = 2.8 \times 10^6$ N/m, radius $\rho = 0.0167$ m and inertia $J = 7.47$ kg m^2. The open-loop system exhibits a beam resonance in the range 55–90 Hz (depending on head position), a transmission resonance at 110 Hz, and the current-regulated motor drives have a bandwidth of 2 kHz. The natural frequencies specified for the reference model are in the 300–400 rad/s range with damping ratio 0.9, whereas for the transmission compensation the natural frequency is chosen to be 1000 rad/s with damping ratio 0.8. The inputs to the prototype are current commands for the three-phase permanent-magnet synchronous motors. Rotary position sensors are located on both motor shafts ($2\pi/40$ mrad resolution), and linear position sensors are located on both gantry joints and on the beam tip (1 μm resolution). The joint position sensor is used for load side feedback, whereas the tip position sensor

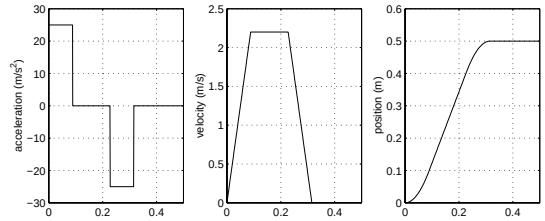

Figure 3: Motion command trajectory.

is used only for monitoring purposes, resulting in colocated control.

The first experiments are intended to reveal the dependence of the RMM controller response on the choice of free parameters α and β. Since these parameters set the location of stable pole-zero cancellations, they have no effect on the response of the ideal rigid-body disturbance-free system. In reality, however, these free parameters will influence the closed-loop response due to both the unmodeled flexible modes of the beam and the friction force disturbance; hence, their proper selection requires some tuning. For the motion reference trajectory $r(t)$ in Fig. 3 and with $\omega_d = 400$ rad/s, the resulting position error responses are displayed in Fig. 4, measured at both the joint and the tip, for several different choices of α and β. In each plot, the steady-state position error is reduced to approximately 1 μm at the joint. Static position errors at the tip of up to 30 μm can be present at steady-state, due to joint clearance. For small values of α and β, the error response exhibits a slow tail that leads to unacceptably large ± 10 μm settling times. For large values of α and β, the slow tail is removed but the error response becomes more oscillatory and structural vibration in the beam is increased. Hence, the choice of free parameters involves a trade-off. The plots show peak joint-tip deflections of around 500 μm, far in excess of the static deflections due to joint clearance. Hence, these plots demonstrate significant structural flexibility effects (either beam flexibility, joint flexibility or some combination), when the placement head is located at the midpoint of the beam.

The next experiments provide a comparison between the RMM controller and the more traditional PID controller. The PID controller is designed to be compatible with the RMM controller, in the sense that two of the three closed-loop poles of the PID control system are selected to match the two poles of the reference model used by the RMM controller, with the remaining pole of the PID control system located where stable pole-zero cancellation occurs in the RMM controller. The result is the gain selection $k_p = M\left(\omega_d^2 + 2\zeta_d\omega_d\gamma\right)$, $k_i = M\omega_d^2\gamma$, $k_d = M\left(2\zeta_d\omega_d + \gamma\right)$, where $\gamma > 0$ is a free parameter. After some manual tuning, it was determined that the most favorable PID controller response was

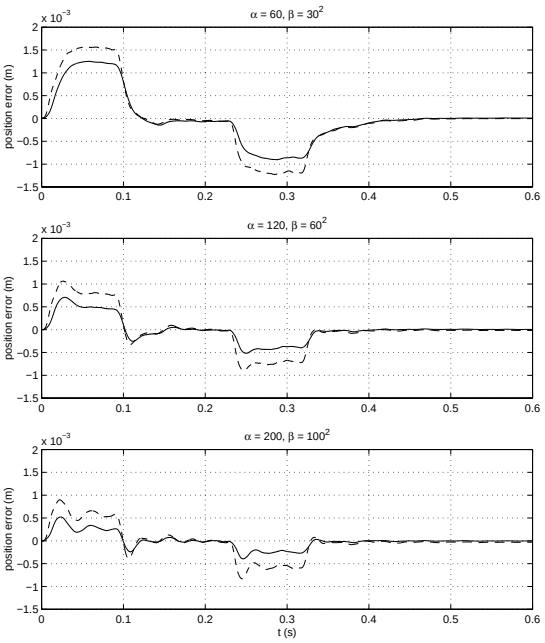

Figure 4: Position errors for RMM controller with x_h at midpoint (— joint error, - - tip error).

obtained using $\omega_d = 300$ rad/s and $\gamma = 100$. The RMM controller used parameters $\omega_d = 300$ rad/s, $\alpha = 200$ and $\beta = 100^2$. Both controllers therefore have adjustable poles placed at $s = -100$. The belt transmission compensation strategy was identical for both motion controllers under comparison, but the motion command trajectory was less aggressive for the PID controller than for the RMM controller due to controller saturation (20 m/s^2 versus 25 m/s^2 and 2.0 m/s versus 2.2 m/s). The results are displayed in Figs. 5 and 6, for head positions near the joint, at the midpoint, and far from the joint. The position error plots in Fig. 5 show that flexibility effects become more significant if the head is located far from the joint. Furthermore, the RMM controller is seen to outperform the PID controller in terms of both joint position error (to some extent) and tip position error (to a large extent). The RMM controller generally appears to achieve the positioning goal more smoothly than the PID controller, which excites significant structural vibration. The q-axis command current, which is proportional to the motor command torque, is shown in Fig. 6 where the smoother behavior of the RMM controller is also apparent.

The comparative experiments just described are summarized in Table 1. Of greatest interest is the ± 10 μm settling time at the placement head and, although this is unmeasured, it may be inferred from the joint and tip settling times which are both directly measured. The PID controller achieves a good settling time if the head is near the joint. For

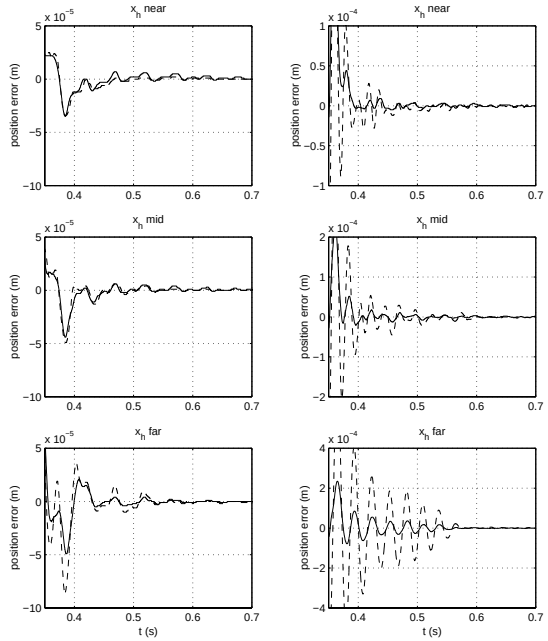

Figure 5: Position error comparison for RMM controller (left column) and PID controller (right column): — joint error, - - tip error.

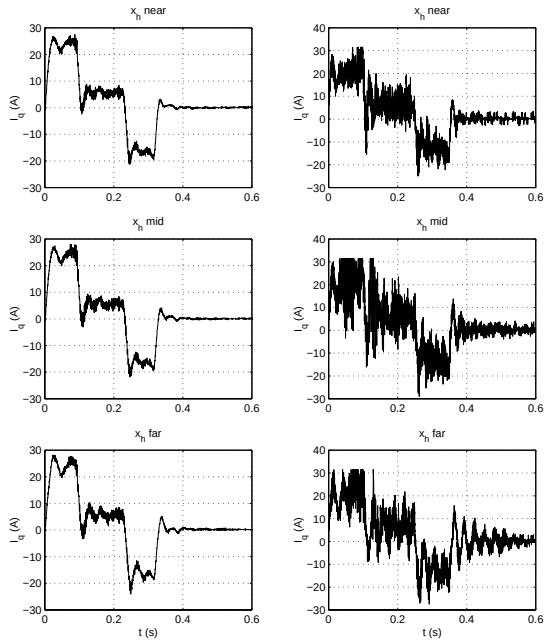

Figure 6: Command current comparison for RMM controller (left column) and PID controller (right column).

controller	x_h near	x_h mid	x_h far
PID design	0.388 s	0.471 s	0.541 s
RMM design	0.432 s	0.435 s	0.424 s

(a) Joint settling time.

controller	x_h near	x_h mid	x_h far
PID design	0.461 s	0.575 s	0.569 s
RMM design	0.412 s	0.440 s	0.472 s

(b) Tip settling time.

Table 1: ± 10 μm settling times.

the more important situation in which the head is located at the midpoint, the RMM controller outperforms the PID controller by 36 ms at the joint and 135 ms at the tip. When the head is far from the joint, the comparison favors the RMM controller even more.

6 Conclusions

This paper has presented a reduced-order model matching controller design based on the LTI rigid-body model of the gantry robot. By placing a compensator pole at the origin, zero steady-state position error is obtained in the presence of large Coulomb friction levels. By adjusting the reference model parameters, the primary features of the closed-loop transient response may be easily tuned. Additional free parameters may be selected so as to favorably influence the extent to which structural vibrations are suppressed. By using feedback to enhance transmission stiffness, faster motion is made possible.

References

[1] C. T. Chen, *Analog and Digital Control System Design*. Fort Worth, TX: Saunders, 1993.

[2] J. Y. Hung, "Control of industrial robots that have transmission elasticity," *IEEE Trans. Industrial Electronics*, 38, 421–427, 1991.

[3] L. Meirovitch, *Principles and Techniques of Vibrations*. Upper Saddle River, NJ: Prentice Hall, 1997.

[4] D. Wang and M. Vidyasagar, "Passive control of a stiff flexible link," *Int. J. Robotics Research*, 11, 572–578, 1992.

[5] X. Yang, D. G. Taylor, N. Nahm and M. Lauzi, "Simulation models for gantry subsystems of SMT placement machines," *Proc. 3rd Int. Symp. Advanced Electromechanical Motion Systems*, Patras, Greece, 971–976, 1999.